Multiple solutions for flow mode−transition in an inclined cavity generated by natural convection

Miloud Zellouf[✉ 1], **Noureddine Moummi**[2], **Adnane Labed**[2], **Kamel Aoues**[1]

1 *Laboratoire de Génie Energétique et Matériaux (LGEM), Université de Biskra, B.P. 145 R.P. 07000, Biskra, Algeria*

2 *Laboratoire de Génie Mécanique (LGM) Université de Biskra B.P. 145 R.P. 07000, Biskra, Algeria*

Received 22 August 2014
Revised 19 August 2015
Accepted 29 February 2016
Published online: 20 December 2016

Keywords
Natural convection
inclined cavity
hysteresis phenomenon
flow mode transition
Sizing calculations

Abstract: An investigation of natural convection in a rectangular cavity (AR = 4) filled with air (Pr = 0.71) heated from the side with adiabatic horizontal walls is carried out numerically. To describe the flow regime, we propose a description of the influence of the angle of inclination and Rayleigh number on the flow patterns likely to develop in this configuration. The numerical analysis of the governing equations of the problem is based on finite volume method with non-staggered grids arrangement and is solved through the iterative SIMPLEC algorithm. Results indicate that the angle of inclination has a significant effect on flow mode transition. The existence of multi-steady solutions closely depends on the value of the Rayleigh number. For that the Hysteresis phenomenon (multi−steady solutions) for Ra ≥ 2000 are demonstrated and parameter maps of Ra vs. ϕ are proposed.

1. Introduction

Natural convection in fluid enclosures has received much attention and extensively studied both experimentally and theoretically (Bodenshatz et al. 2000). The interest in this class of flows has been motivated by diverse engineering problems. It is the result of complex interaction between finite−size fluid systems in thermal communication with all the walls that confine it. The thermal convection in inclined cavities represent the typical behavior of many physical systems (e.g., collection of solar energy such as solar collectors, storage devices, operation and safety of nuclear reactors, effective cooling of electronic components and machinery, energy efficient design of buildings and rooms, double or multi−pane slope windows and skylights, material processing equipment such as melting and crystal growth reactor) (See Huppert and Turner 1981 and Turner 1985).

Most of published research in this field that exit until today can be classified into two groups:

i) differentially heated enclosures (conventional convection) and ii) enclosures heated from below and cooled from above (classical Rayleigh−Bénard convection), (See also Ostrach 1972 and Catton 1978). The natural convection in inclined enclosures combined the two class of flows mentioned above with special interest because the associated flow mode−transition and hysteresis phenomenon (dual or multi−steady solutions) in a 2−D heated inclined enclosure, that had been observed and reported by many researchers:

Although experimental studies, Hart (1971), Hollands and Konicek (1973), Ozoe et al. (1975), Arnold et al. (1976) and Hamady et al. (1989), it is found that, the heat transfer decreases and reaches its lowest value, and then gradually increases again when the tilt angle changes from 0° to 90°. The minimum point occurs at the angle where the flow changes its mode from the three-dimensional roll pattern (caused by the thermal instability) to the two-dimensional circulation (caused by the hydrodynamic effect). These research studied cavities with small to medium aspect ratios, with maximum aspect ratio of 15.5, except the study of Hollands and Konicek (1973) that have used an enclosure with aspect ratio equal to 44. In the study of Elsherbiny et al. (1982) and Elsherbiny (1996), six aspect ratios between 5 and 110 were experimentally examined to find the influence of the tilt angle and the aspect ratio on the heat transfer rate. A correlation for tilt angle 60° was developed.

Many numerical studies were also performed to solve the problem of natural convection in inclined enclosures. Soong et al. (1996) in order to investigate the effect of inclination angle from 0° to 90° on flow mode−transition in an inclined rectangular enclosure heated from below and cooled from above with two insulated side walls. Different aspect ratios were considered (AR = 1, 3 and 4) with Rayleigh number ranged from 1.5×10^3 to 2×10^4, flow mode−transition and hysteresis phenomenon for Ra>2000 were demonstrated. In addition hysteresis effect were also reported by Corcione (2003), thus confirming that bidirectional differential heating with various thermal conditions imposed on

✉ Corresponding author. E-mail address: zellouf_miloud@hotmail.com

Nomenclature

AR	aspect ratio, H/L
g	gravitational acceleration [m s $^{-2}$]
H	height of the side wall [m]
L	length of the side wall [m]
Nu	mean Nusselt number
P	pressure [Kg m^{-1} s^{-2}]
Pr	Prandtl number, ν/α
Q	error in energy balance
Ra	Rayleigh number, $\rho g\beta(T_h-T_c)H^3/\alpha\mu$
T	temperature [k°]
$\vec{U}$	vector of velocity
u, v	dimensionless velocity components
x, y	dimensionless coordinates
%	value of percent deviation

Greeks symbols

α	thermal diffusivity [m^2 s $^{-1}$]
β	coefficient for thermal expansion [k° $^{-1}$], $-(\partial\rho/\partial T)_P/\rho$
$\vec{\delta}$	cosines director $\vec{\delta} = \sin(\phi)\vec{\imath} + (\phi)\vec{\jmath}$
Δ	Laplacian operator $\Delta = \nabla^2 = (\partial^2/\partial x^2) + (\partial^2/\partial y^2)$
$\vec{\nabla}$	Nabla operator, $\vec{\nabla} = (\partial/\partial x)\vec{\imath} + (\partial/\partial y)\vec{\jmath}$
θ	dimensionless temperature function, $(T-T_c)/(T_h-T_c)$
μ	kinematic viscosity [kg m^{-1} s^{-1}]
ν	kinematic viscosity [m^2 s^{-1}]
ρ	fluid density [kg m $^{-3}$]
ϕ	(Phi) inclination angle [deg]
ψ	dimensionless stream function
ω	dimensionless vorticity.

Subscripts

c	cold wall or critical
h	hot wall
H	horizontal wall
V	vertical wall
max	maximum
min	minimum
0	related to the mean temperature
$\rightarrow$	related to the vector value

the side walls of the cavity, has a significant effect on flow mode-transition of natural convection inside horizontal enclosures heated from below and cooled on the top. Wang and Hamed (2006) also, carried out a numerical investigation on the effect of some heating configurations that was previously considered by Corcione (2003), they combined the cavity inclination angle of flow-pattern of natural convection that was reported by Soong et al. (1996) with imperfect thermal boundary conditions in rectangular enclosure with single aspect ratio of 4.

Recently Khezzar et al. (2012) investigated numerically the flow structure and heat transfer behavior due to natural convection in enclosures of aspect ratios 1, 3, 6 and 12 for Ra = 10^4, 10^5 and 10^6 and for inclination angles between 0° and 180° and (Pr = 10). The flow−mode transition and the Nusselt variation with the inclination angle have been presented.

More recently, Chang (2014) carried out a numerical study of two-dimensional natural convection in differentially heated enclosure, in order to investigate the effect of the aspect ratio and inclination angle on flow and heat transfer for (AR = 1, 2, 4 and 8, 0°≤ ϕ ≤ 180° and Ra = 10^3, 10^4, 10^5 and 10^6 with Pr = 0.71), moreover many correlations for average heat transfer in horizontal (ϕ = 0°) and vertical (ϕ = 90°) configuration are proposed.

In our laboratories, there have been many investigations on the natural convection in confined enclosures (Labed et al. 2005, Aoues et al. 2007 and Zellouf et al. 2014), and many contributions on the enhancement and testing of thermal performances of solar FPCs designed for heating, cooling and drying applications, e.g. (Moummi et al. 2004, Moummi et al. 2010, Aoues et al. 2011, Labed et al. 2012, 2013, 2014 and 2015). In all these studies, the authors studied the heat transfer the air channel duct. The aim of the present paper is to investigate the natural convection in an inclined rectangular cavity heated from below with insulated vertical walls (at ϕ = 0°). The study is conducted numerically under the assumption of steady laminar flow, the Rayleigh number based on the cavity width in the range between 10^3 and 10^4, and the inclination angle changes from horizontal to vertical position, whose effect on the flow patterns formation, the heat transfer rates and the temperature distributions are examined. Hysteresis phenomenon occurring in the inverse courses of inclination is also studied. Parameter maps of Ra vs. ϕ are proposed, in which flow patterns characterized by various mode are designated.

2. Mathematical formulation of the problem

The geometry and computational domain considered in the proposed model are depicted schematically in Fig. 1 and Table 1. A two-dimensional Cartesian coordinate system is selected such that the y-axis points positively upwards while the gravitational force acts downwards. The rectangular enclosure of height (H) and length (L) filled with air is differentially heated on a sidewall, while the other opposite wall is kept at uniform cold temperature. The top and bottom sidewalls are assumed adiabatic (at ϕ = 90°), and can be rotated around the horizontal axis (x). Each configuration is defined by the angle of inclination.

2. 1. Governing equations

The buoyancy−driven flow is considered to be 2D−steady and laminar. The fluid is assumed incompressible, with constant physical properties and negligible viscous dissipation. The buoyancy effects upon momentum transfer are taken into account through the Oberbeck−Boussinesq approximation (see Oberbeck 1879, Boussinesq 1903 and Zeytounian 2003).

Once the above assumptions are considered for solving the conservation equations of mass, momentum and energy, we can write the dimensionless governing equations as follows (see Jaluria 1980):

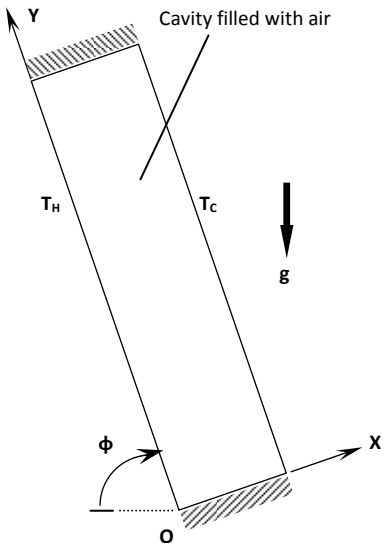

Fig. 1. Physical model, boundary conditions and the coordinate system of problem.

Table 1. Summary of geometric and model parameters.

	Fixed parameters	Variable parameters
Geometric parameters	AR = 4 (H = 4, L = 1)	ϕ = 0° - 90°
Ranges of model parameters	Pr = 0.71	Ra = 10^3 - 10^4

The equation of continuity:

$$\vec{\nabla}.\vec{U} = 0 \tag{1}$$

The equations of motion are given by:

$$(\vec{U}.\vec{\nabla}).\vec{U} = -\vec{\nabla}P + \Delta\vec{U} + Pr^{-1}Ra\theta.\vec{\delta} \tag{2}$$

The equation of energy is as follows:

$$\vec{U}.\vec{\nabla}\theta = Pr^{-1}\Delta\theta \tag{3}$$

Where:

$\theta = (T - T_c)/(T_h - T_c)$: the temperature function,

$\vec{\delta} = \sin(\phi)\,\vec{\imath} + \cos(\phi)\,\vec{\jmath}$: the cosines director,

$Ra = \dfrac{\rho g \beta (T_h - T_c) H^3}{\alpha \mu}$: the Rayleigh number,

$Pr = \dfrac{\nu}{\alpha}$: the Prandtl number, set to 0.71.

The well−known Oberbeck−Boussinesq approximation is employed, i.e., those physical properties are constant except for the density in the buoyancy term, which is assumed to vary with temperature only according to:

$$\rho = \rho_0\,[1 - \beta(T - T_0)]$$

Where:

$\beta = \left[\frac{1}{\rho}\left(\frac{\partial \rho}{\partial T}\right)\right]_P$: is the coefficient for thermal expansion.

2. 2. Boundary conditions

The left and right walls are maintained at constant temperatures; hot temperature ($\theta = 1$) is applied to the left sidewall while the other right wall is kept at uniform cold temperature ($\theta = 0$). The remaining walls are assumed insulated from the surrounding. Thus, the boundary conditions (in vertical position $\phi = 90°$) are as follows:

$$\left.\begin{array}{l} u = v = 0 \quad \text{at four walls} \\ \partial\theta/\partial y = 0 \ \text{ at } \ y = 0 \ \text{ and } \ y = AR \\ \theta = 1 \ \text{ at } \ x = 0 \ \text{and} \ \theta = 0 \ \text{at} \ x = 1 \end{array}\right\} \tag{4}$$

Where AR = H/L, is the height−to−length aspect ratio of the enclosure, set to 4.

No slip boundary condition (u = v = 0) is imposed at the four walls of the cavity. Two side walls are thermally insulated, whereas the other two opposite walls are kept at the uniform temperatures (T_h) and (T_c), respectively.

3. Computational procedure

3. 1. Numerical algorithm

The above system of equations (1–3) with the boundary conditions (4) is solved through a control-volume formulation based of the finite-difference method. The pressure-velocity coupling is handled by using the SIMPLE−C algorithm (Van Doormaal and Raithby 1984), which is essentially a more implicit variant of the SIMPLE algorithm proposed by Patankar and Spalding (1972). The convective fluxes across the surfaces of the control volumes are evaluated by using the power−law discretization scheme, recommended by Patankar (1980). The discretized governing equations are solved iteratively through a line−by−line application of the Thomas algorithm. Under−relaxation is used to ensure the convergence of the iterative procedure.

3. 2. Domain discretization

The computational domain is covered with a non-equidistant grid, having a concentration of grid lines near the boundary surfaces and a uniform spacing in the interior of the cavity. Furthermore, since multi-cell flow structures are expected, especially at the largest height−to−length aspect ratios investigated, and the location of the cell interfaces is not known a priori, a fine mesh spacing is used everywhere in the vertical direction. The solution is considered to be fully converged when the maximum absolute value of the mass source and the percent changes of the dependent variables at any grid−node from iteration to iteration are smaller than a prescribed value, i.e., 10^{-6} and 10^{-8}, respectively. In addition, the percent difference between the in-coming and out-coming heat transfer rates is used as a further indication of the accuracy of the solution achieved. After convergence is attained, the average Nusselt number Nu_H of each horizontal boundary wall and the average Nusselt number Nu_V of each vertical boundary wall are calculated:

$$Nu_H = \int_0^1 \left.\frac{\partial\theta}{\partial y}\right|_{wall} dx \quad \text{and} \quad Nu_V = \frac{1}{AR}\int_0^{AR} \left.\frac{\partial\theta}{\partial x}\right|_{wall} dy \tag{5}$$

3. 3. Grid dependence test

In thermal convection problems grid density strongly depend on Rayleigh number. For an inclined enclosure, grid density also depends on flow patterns, which in turns strongly depend on the

cavity angle of inclination. A grid dependence test was performed for Rayleigh number in the range between 10^3 and 10^4. For each model, grid test was performed at seven angles of inclination; 0°, 15°, 30°, 45°, 60°, 75° and 90°. A sample of the results of this grid dependence test of the average Nusselt number at the cavity cold wall, the maximum velocities u_{max} and v_{max}, and the error in energy balance Q_{error} at Ra = 10^4 is listed in Table 2. The 62×242 grid was found appropriate for all configurations considered in the present study. Results of grid dependence test for inclination angles (ϕ) = 0°, 30°, 60°, 90° degree at Ra = 10^4. Values between brackets indicate absolute percent difference to the 62×242 grid.

3. 4. Numerical calculations

Since mode transition is very sensitive to the initial conditions or initial guess as indicated in Hart (1971), Hollands and Konicek (1973), and the investigation of the hysteresis phenomenon is one of the major objectives of the present study, the sequence used to carry out the numerical calculations will be specified clearly. In calculations of the case of ϕ increasing from 0° to 90°, flow and temperature fields at a constant Ra and ϕ = 0° are first calculated using 0 as initial guess for the velocity and the temperature fields. The ϕ = 0° solution is then used as initial condition for solution of the subsequent case of inclination with ϕ = 5°, which is then used as an initial condition for the subsequent case of ϕ = 10°, and so on. As the value of ϕ at which mode-transition occurs is determined, say between 30° and 35°, calculations are then repeated starting from 30° with increments of 1° in order to locate mode−transition angle within 1° accuracy. A similar procedure is employed for calculations with ϕ decreasing starting from 90° back to 0°, using the 90° solution obtained from the ϕ increasing case as an initial condition for ϕ = 85°and so on.

In order to check the accuracy of the results obtained using the present numerical algorithm, results were compared with those available in the literature. Numerical results of flow and thermal fields and average Nusselt numbers obtained at Ra = 10^4, AR = 4,

Pr = 0.71, and ϕ between 0° to 90° were compared and found in good agreement with those reported in Soong et al. (1996), Corcione (2003) and Wang and Hamed (2006).

4. Results and discussion

Numerical simulations are performed for Pr = 0.71 (air is the working fluid) for different values Rayleigh number ($10^3 \leq Ra \leq 10^4$) and cavity inclination angle (0°≤ ϕ ≤ 90°). In order to point out the influence of Ra and ϕ upon the flow structure type and the temperature distributions throughout the cavity, sample local results are reported in terms of isotherms and streamlines. In all the isotherm plots, the contour lines correspond to equi–spaced values of the dimensionless temperature θ in the range between 0 and 1. In all the streamline plots, the contour lines correspond to equi–spaced absolute values of the normalized dimensionless stream function ψ in the range between 0 and 1, where the dimensionless stream function ψ is defined as usual through: $u = \partial \psi / \partial y$ and $v = -\partial \psi / \partial x$.

4. 1. Heat transfer rates

The mean heat transfer rates (Nu) at various Rayleigh numbers and inclination angles (ϕ) from 0° to 90° are presented in Fig. 2. For zero-inclination, the critical Rayleigh number is about 1708, Nu is still kept as 1.0 for subcritical ($Ra < Ra_C$) state, where no convection was observed and conduction was the dominating mode of heat transfer. As the enclosure is tilted, the upward buoyant flow along the upslope wall is built.

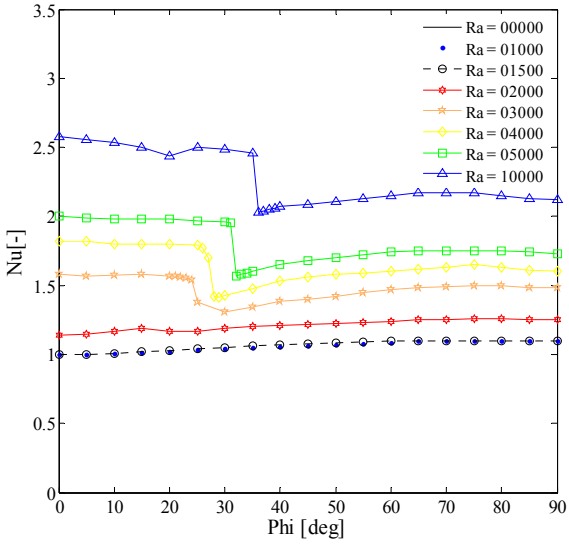

Fig. 2. Average Nusselt numbers at various ϕ and Ra.

Table 2. Results of grid dependence test for inclination angles (ϕ) = 0°, 30°, 60°, 90° degree at Ra = 10^4. Values between brackets indicate absolute percent difference to the 62×242 grid.

Angle (ϕ)	Nombre of grid points	Nu-cold wall	(%)	v_{max} × 10^{-4}	(%)	u_{max} × 10^{-4}	(%)	Q_{error}
00°	32X122	1.55	(1.31)	26.8	(1.52)	72.5	(1.49)	0.39
30°	32X122	1.79	(1.13)	22.1	(1.38)	69.5	(1.84)	0.50
60°	32X122	2.09	(0.48)	27.1	(1.50)	56.3	(1.23)	0.56
90°	32X122	2.47	(0.00)	45.0	(2.39)	40.9	(3.99)	0.49
00°	62X242	1.53	(0.00)	26.4	(0.00)	73.6	(0.00)	0.16
30°	62X242	1.77	(0.00)	21.8	(0.00)	70.8	(0.00)	0.17
60°	62X242	2.08	(0.00)	26.7	(0.00)	57.0	(0.00)	0.17
90°	62X242	2.47	(0.00)	46.1	(0.00)	42.6	(0.00)	0.15
00°	92X362	1.53	(0.00)	26.4	(0.00)	73.5	(0.14)	0.12
30°	92X362	1.77	(0.00)	21.7	(0.46)	70.8	(0.00)	0.12
60°	92X362	2.08	(0.00)	26.7	(0.00)	57.2	(0.35)	0.12
90°	92X362	2.47	(0.00)	46.2	(0.22)	42.7	(0.23)	0.11

The heat convection contributes gradually, and the Nu departs from the conduction state (Nu = 1). For a higher Rayleigh number, Ra = 2000, which lies at a supercritical ($Ra > Ra_C$) state, Nu for $\phi = 0°$ is around 1.1, the convection contributed immediately as evident by the value of Nusselt number.

As Ra further increased, e.g. Ra = 3000, 4000, 5000 or 10000, a noticeable drop in Nusselt number appeared as (ϕ) was increased. This drastic change in the rate of heat transfer implied a mode−transition of the flow pattern.

4. 2. Flow−mode transition

The evolution of flow structure and temperature field illustrates by the contour lines of ψ and θ for the range $10^3 \leq Ra \leq 10^4$ in Figs. 3−7.

In Fig. 3, Ra = 1000, the fluid in this subcritical ($Ra < Ra_C$) state is still regarded as stationary. As the enclosure is inclined, $\phi = 1°$, the shear flow along the two longitudinal walls results a large circulation in which there are two weak sub−cells rotating in the same sense as the primary cell. This two cellular mode disappears at ϕ between 48° and 50° due to stronger up−slope/down−slope flows along the x−direction.

For $\phi \geq 50°$, the flow pattern is one cell mode, a similar evolution behaviour with almost the same values are presented in Fig. 4 for Ra = 1500. The isotherms lines in Fig. 3 and Fig. 4 illustrate a gradual change from a stratification state to a skew−symmetric distortion due to the cellular motion.

Figure 5 shows the case of Ra = 2000, in which the flow appears as a four−cell structure at $\phi = 0°$. In this slightly super−critical state ($Ra > Ra_C$), the cellular motion of flow pattern is weak, the left−most cell at the upper end of the inclined enclosure cannot resist the upward flow coming from the hot wall and, then, it is smeared out at $\phi \leq 2°$.

Hereinafter, the flow structure turns to the three−cells and the isotherms show the attendant change in temperature field. As the inclination angle increases, the flow pattern changes to a two−in−one cell mode at $\phi = 15°$, and the latter structure persists until $\phi = 44°$.

At $\phi = 45°$, the flow pattern turns to one-cell mode. For a relatively higher Rayleigh number, Ra = 5000 in Fig. 6, the cellular motion of flow pattern becomes relatively stronger due to larger buoyancy, hence the four−cells structure can maintain for inclination angle up to $\phi = 13°$. The flow pattern turns to a three−cells structure at $\phi = 14°$ and retains the same pattern up to $\phi = 30°$. Subsequently, the one cell mode prevails in the range of $31° \leq \phi \leq 90°$.

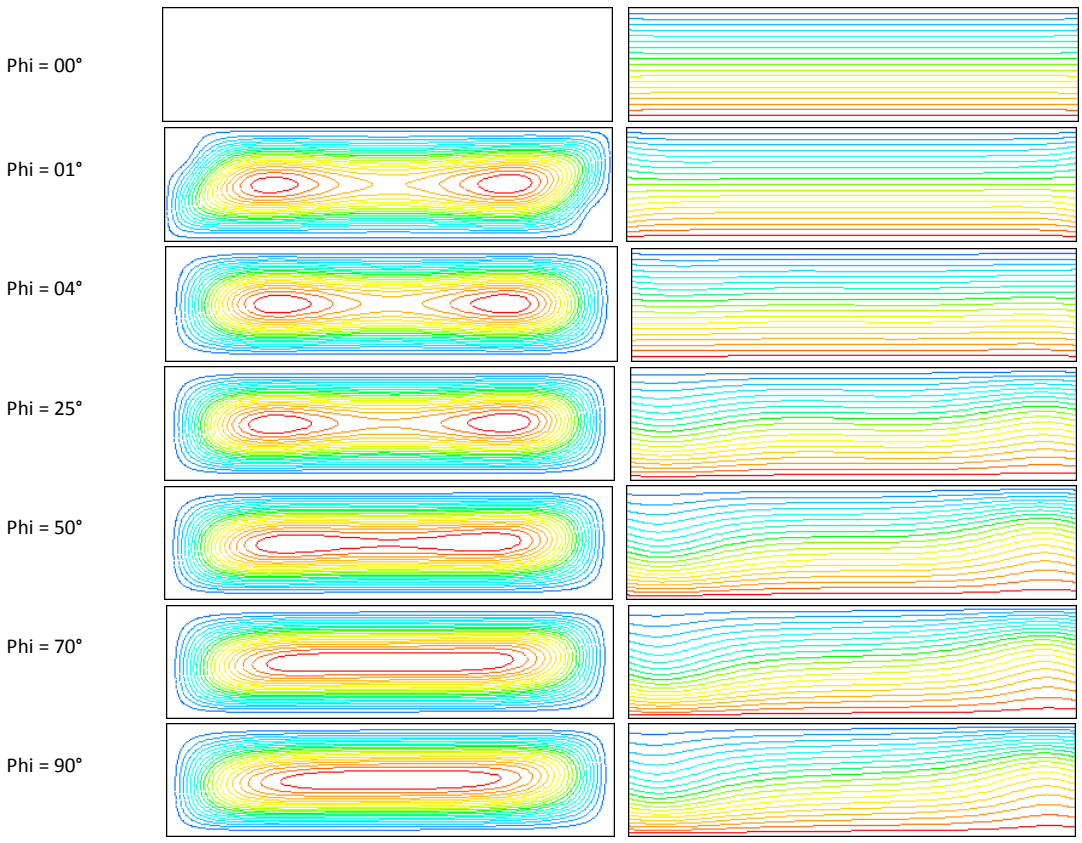

Fig. 3. Streamlines (left column) and isotherms (right column) for Ra = 1000 and ϕ increasing.

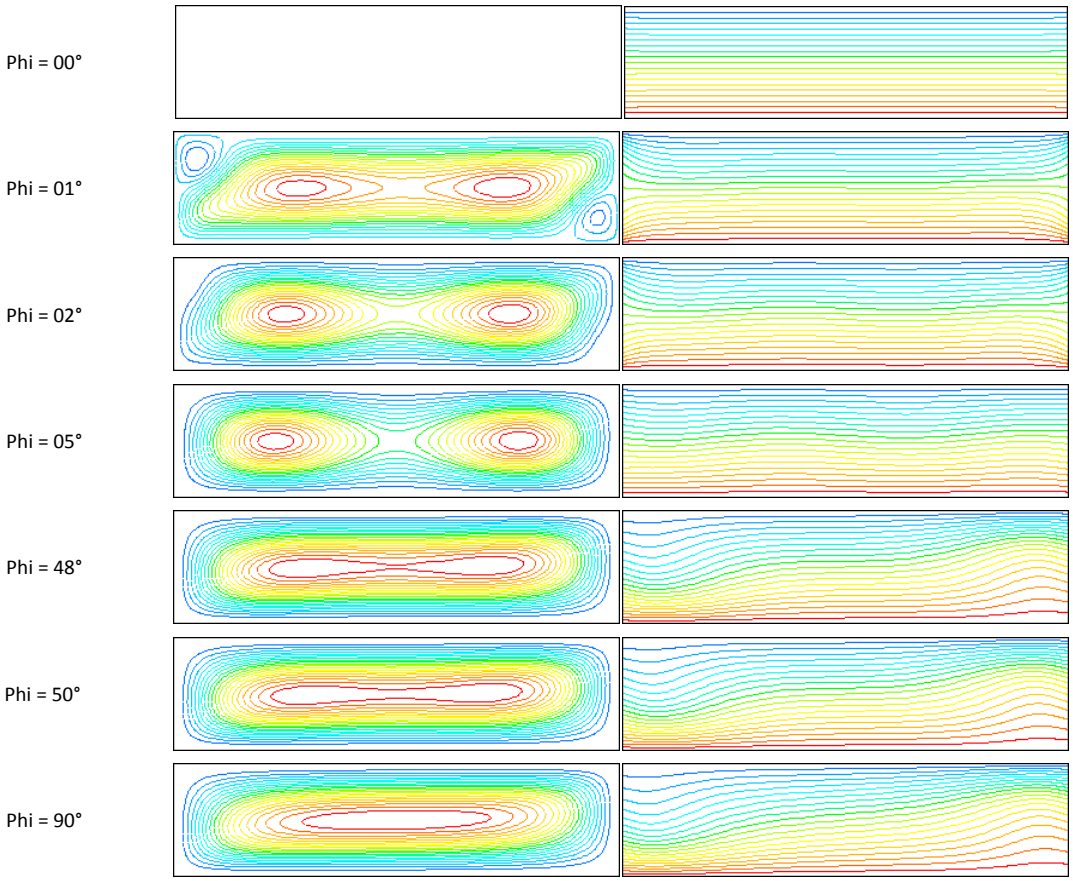

Fig. 4. Streamlines (left column) and isotherms (right column) for Ra = 1500 and ϕ increasing.

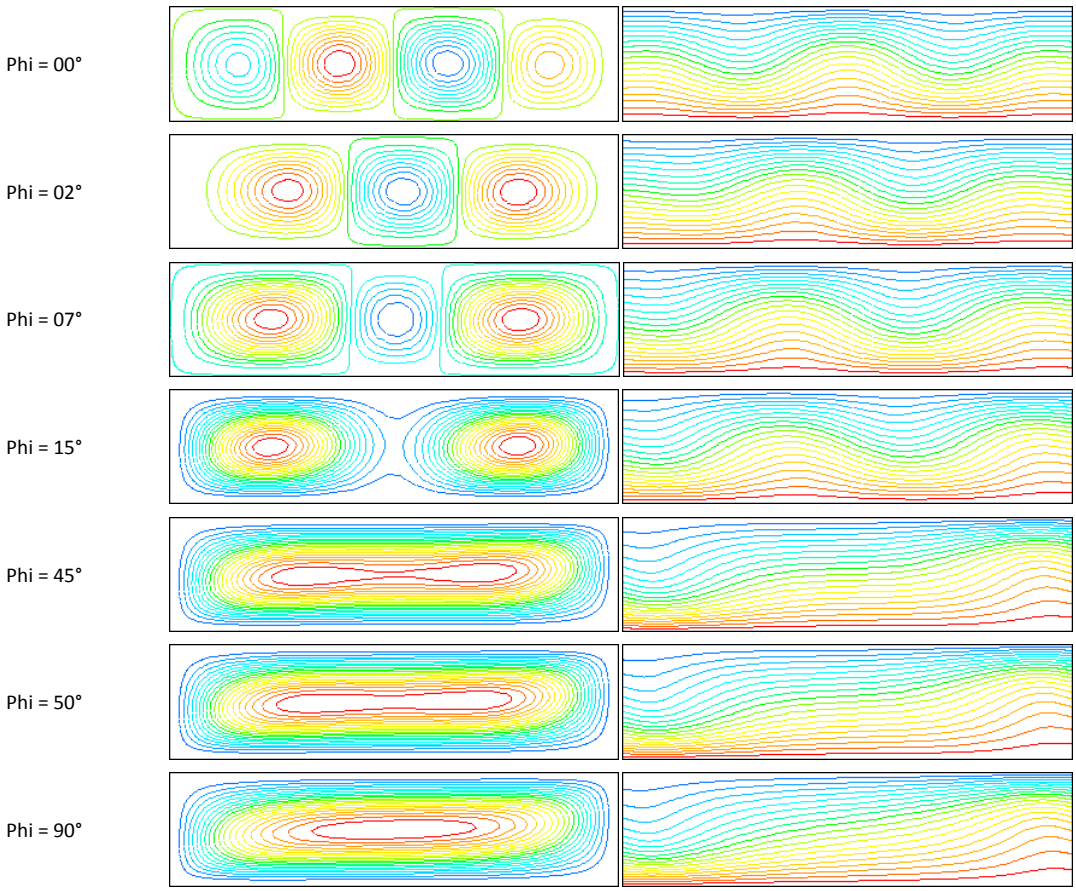

Fig. 5. Streamlines (left column) and isotherms (right column) for Ra = 2000 and ϕ increasing.

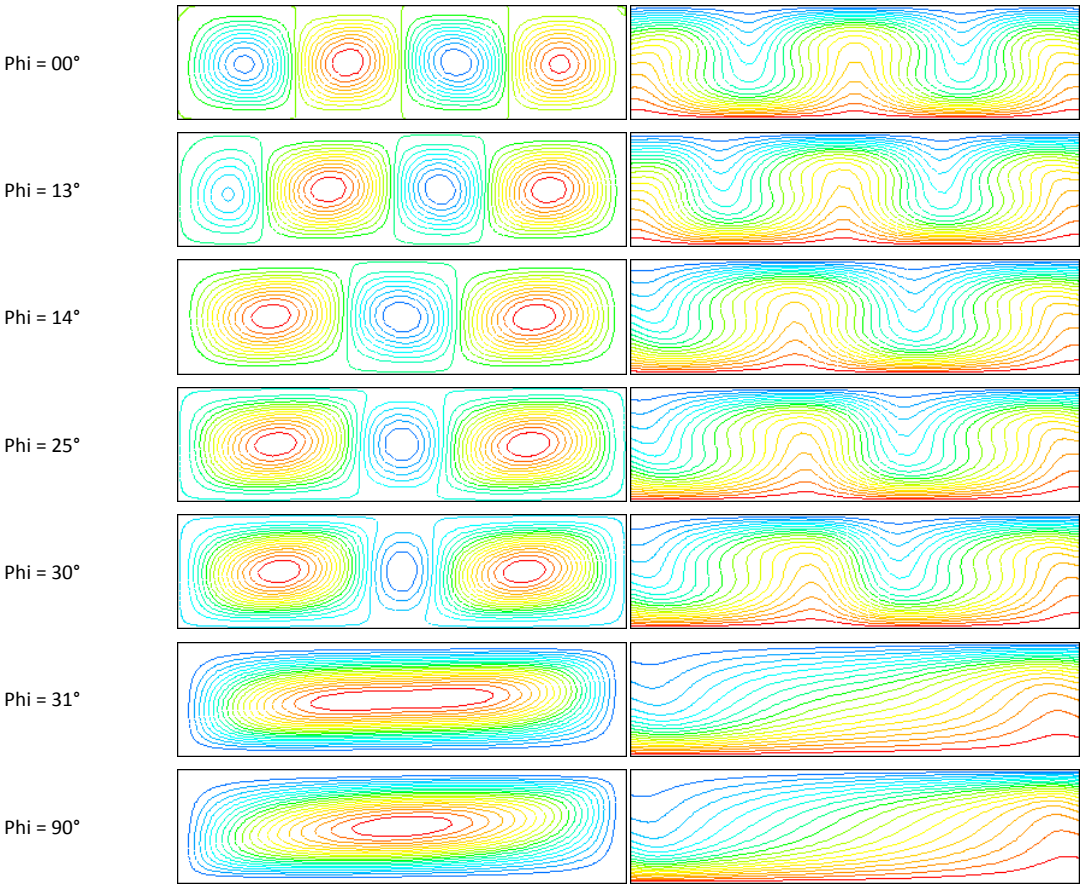

Fig. 6. Streamlines (left column) and isotherms (right column) for Ra = 5000 and ϕ increasing.

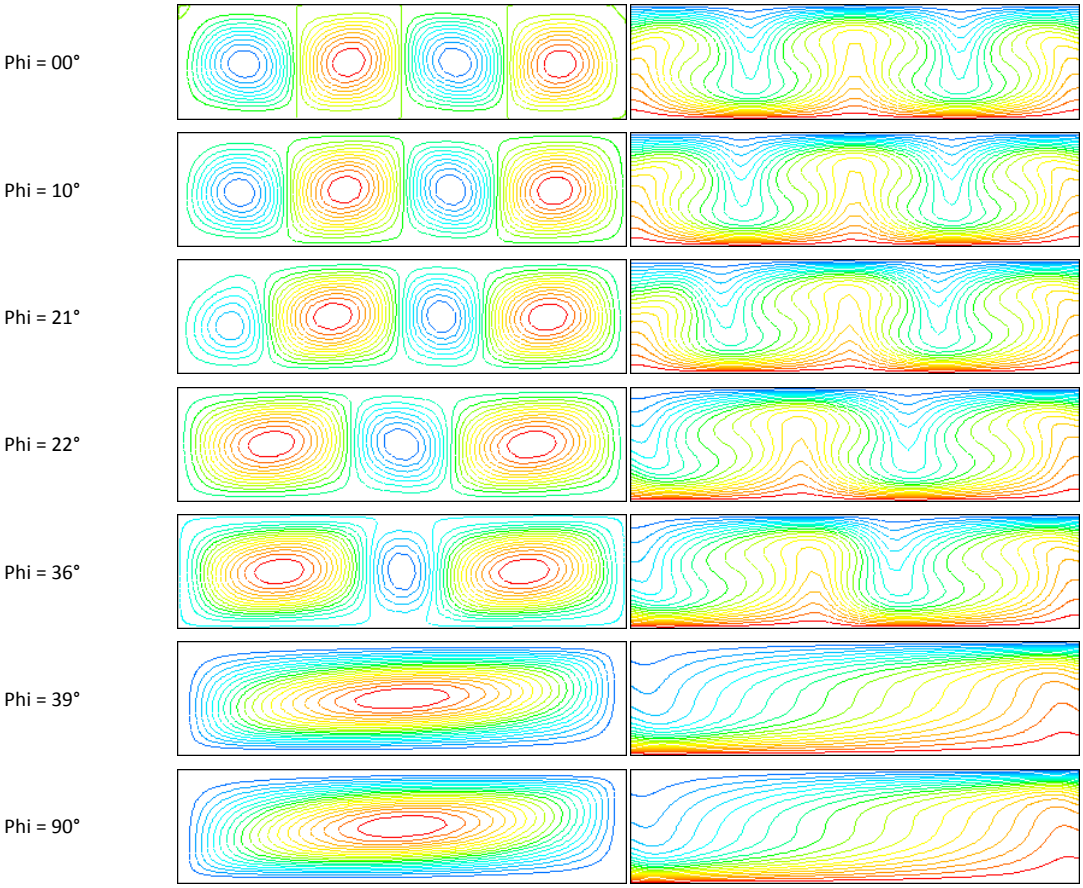

Fig. 7. Streamlines (left column) and isotherms (right column) for Ra = 10000 and ϕ increasing.

The isotherms change from a highly-distorted state for multi−cells structures at low-ϕ to a simple pattern for one−cell mode at ϕ ≥ 31°. As the Rayleigh number further increases, the occurrence of the flow mode−transition from four−cells to three-cells can be postponed to a higher value of ϕ, e.g. ϕ = 22° for Ra = 10000 in Fig. 7. Also, in the high−Ra case, the mult−cells flow pattern turns to one cell mode at a higher inclination (ϕ = 39°).

4. 3. Hysteresis phenomenon

The exits of multiple solutions are possible, where caused by the nonlinear nature of the problem. To investigate the hysteresis phenomenon, the course of the computations are reversed, in Fig. 8 shows the comparisons of the calculated mean Nusselt numbers for increasing and decreasing ϕ. For Ra < 2000, no significant difference between the results obtained in the two courses of changing ϕ. At Ra = 2000, two solutions deviate in a small region of inclination in the range of ϕ < 10°. For a higher Rayleigh number, Ra = 5000, an additional hysteresis region near ϕ = 30° emerges and the two dual−solution regions enlarge with increasing Ra. As Ra further increases to Ra = 10000, the hysteresis prevails in a considerable range of lower inclination.

The bifurcation point moves toward high ϕ as Ra increases. It implies the complexities of the flow field at high heating rates. As an illustrative example of the hysteresis phenomena, the mode transition of the flow and temperature fields at Ra = 10000 and with ϕ−decreasing are shown in Fig. 9 and compared with those for ϕ increasing in Fig. 7. Comparison shows that the flow−mode transition can be significantly influenced by the course of changing inclination ϕ.

4. 4. Parameter maps

The parameter maps can be very useful tools in summarizing the flow patterns for various combinations of the parameters involved and controlled the system. In the present work, only the enclosure of AR = 4 is considered as a typical example to illustrate the diversity of the flow structure and the difference in parameter maps for the ϕ−increasing and ϕ−decreasing courses.

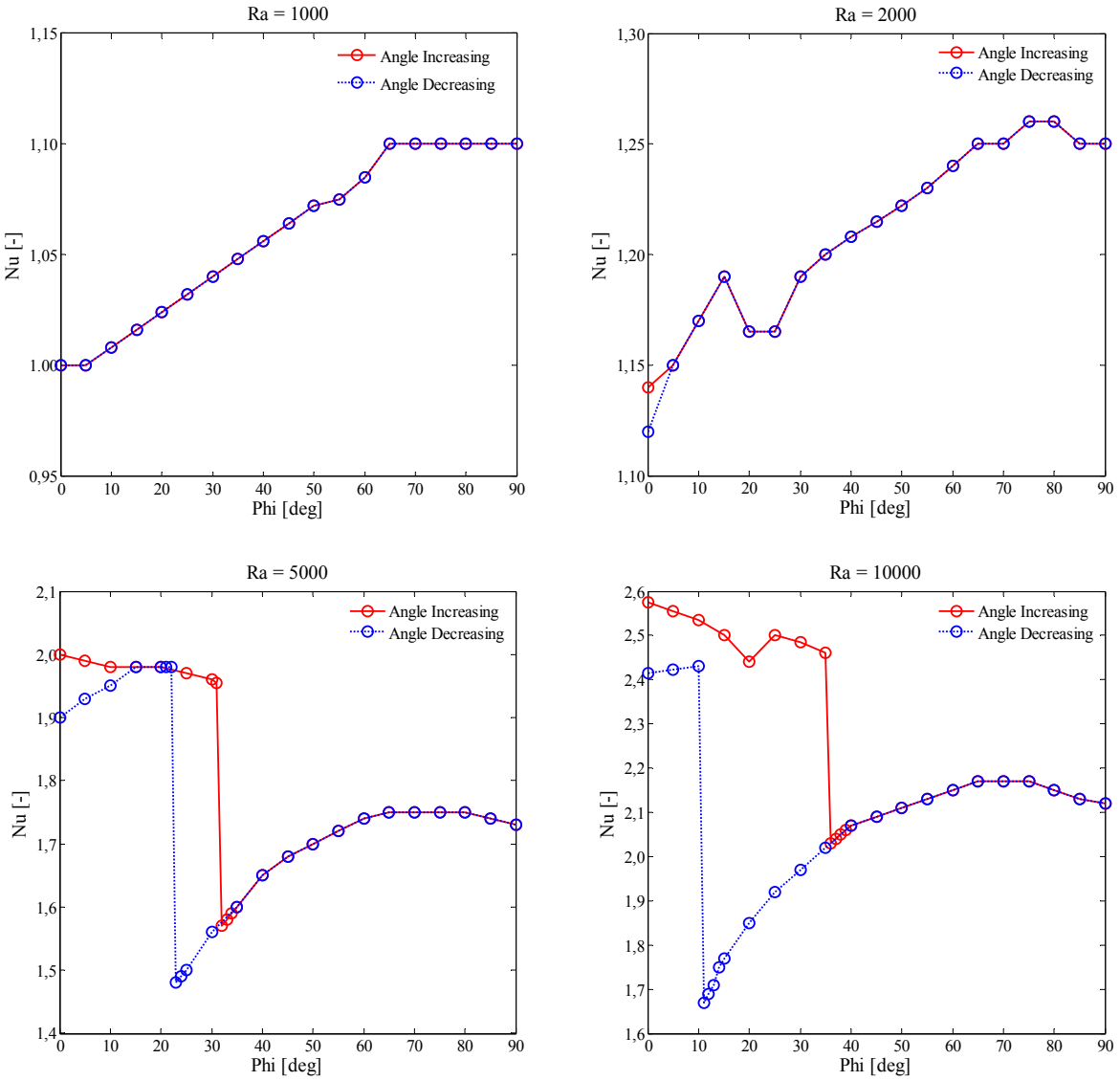

Fig. 8. Hysteresis phenomena denoted by average Nusselt numbers at various Rayleigh numbers for the case of angle increasing and decreasing.

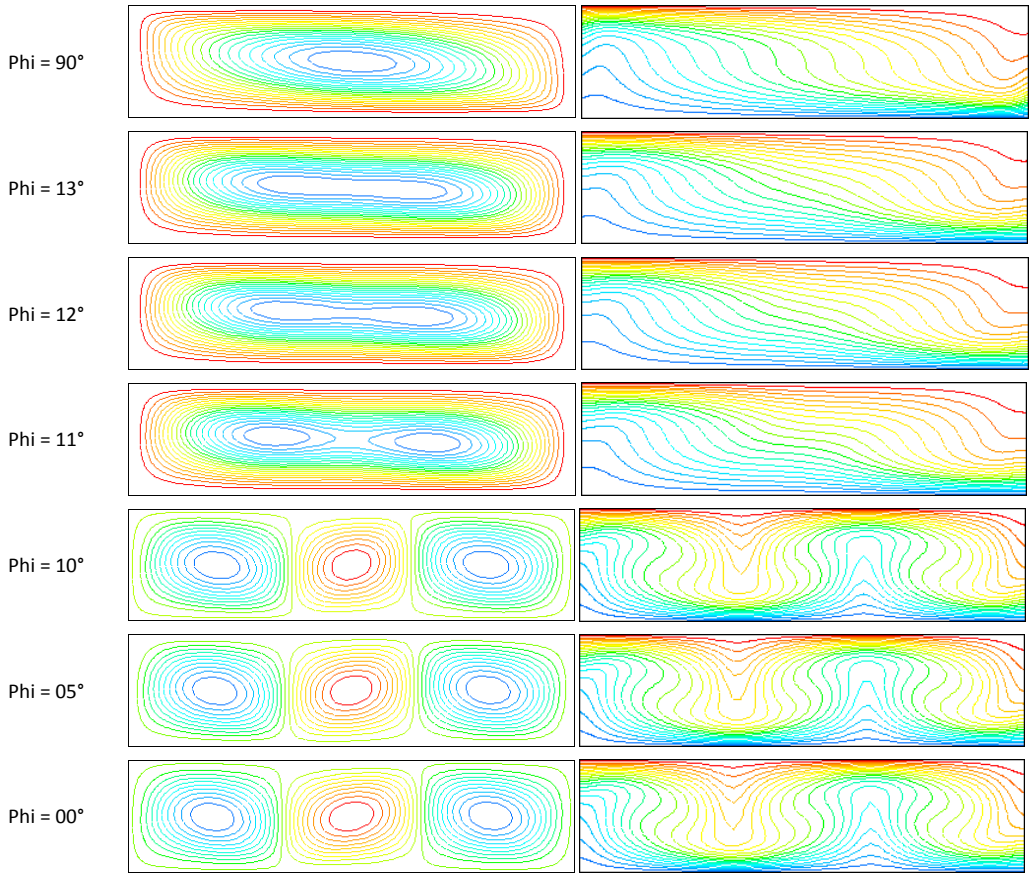

Fig. 9. Streamlines (left column) and isotherms (right column) for Ra = 10000 and ϕ decreasing.

In Fig. 10 (a) for ϕ−increasing, the multi-cell structures exist in low−ϕ cases, in which the thermal instability mechanism dominates. With increasing Rayleigh number, the flow regimes of multi-cell structures become large. It is also attributed to the dominant role of the convection cells, while for the high inclination, the one cell mode is prevailing due to the strong upslope flow along the hotter isothermal wall caused by large buoyancy force component in that direction. The strong longitudinal flow destroys the multi-cell structures.

In Fig. 10 (b) for ϕ−decreasing, the flow mode transition is distinct from that for ϕ−increasing. Since the flow field at large inclination angles are of simple one cell structure, the flow tends to maintain the one cell structure as ϕ decreases from 90°.

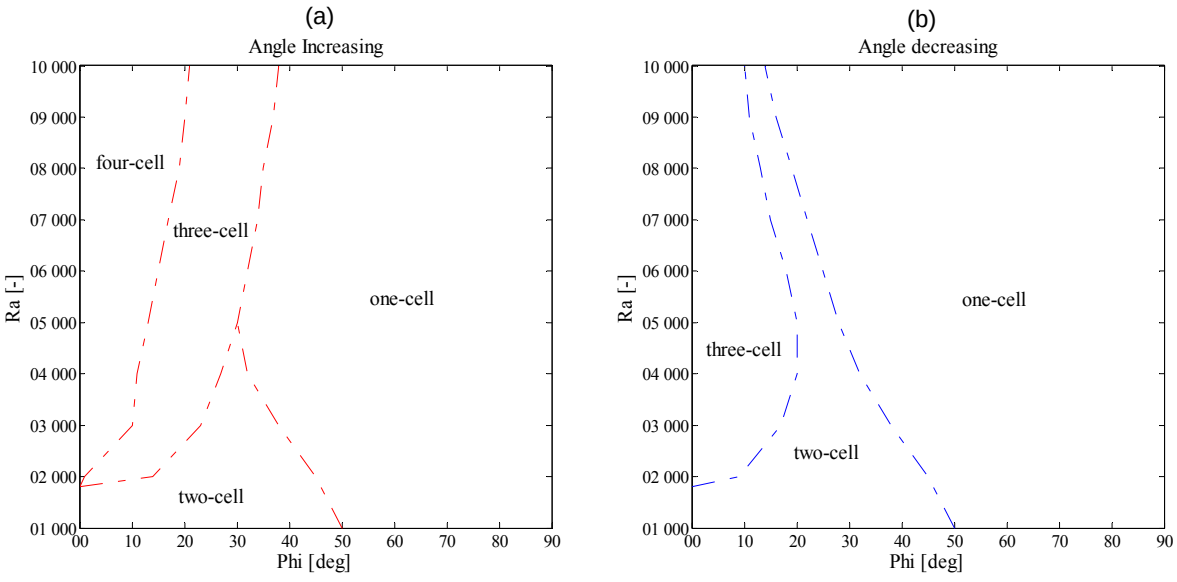

Fig. 10. Parameter maps for natural convection in two-dimensional inclined enclosure for the case of AR = 4 with angle (a) increasing and (b) decreasing.

Therefore, a larger one cell region is shown in the parameter map. Similarly, the simple structure of two−in−one cell can exist at the lower ϕ, especially in the cases of high Ra. Relatively, the complex flows of the three−cell structure are restricted in a smaller regime, and the four-cell mode even disappears in this ϕ−decreasing course.

5. Conclusion

A numerical study of natural convection in a 2−D differentially heated rectangular cavity (AR = 4) is carried out, in order to investigate the effect of Rayleigh number and inclination angle on flow and heat transfer over the range $0° \leq \phi \leq 90°$ and $10^3 \leq Ra \leq 10^4$.

The results showed that the calculation program leads to consistent results and very good agreement with experimental and simulation data in the literature. The possible flow patterns are four-cells, three-cells, two-in-one cell and one cell. For a fixed value of Ra, the transition of the flow mode strongly depends on the competition of the buoyant flow and the shear flow due to inclination.

The occurred heat transfer has a close relationship with the flow structure transition, a sudden decrease in Nu occurred when three-cells or two-in-one cell structure changed into a single cell. The multi-cells structures can exist at low inclination angles, Nu reached its maximum value at ϕ = 0° for all Ra >2000. Hysteresis phenomenon appeared when ϕ decreased from 90° to 0°, and the flow pattern maps are different when ϕ increased, in the process of changing from a single cell to a multi cells structure.

References

Aoues, K., A. Labed, M. Zellouf, N. Moummi (2007) Convection with double diffusion in a rectangular cavity agitated by parallel gradients, Int. Conference on Modelling and Simulation, Algiers.

Aoues, K., N. Moummi, M. Zellouf, A. Benchabane (2011) Thermal performance improvement of solar air flat plate collector: a theoretical analysis and an experimental study in Biskra, Algeria. International Journal of Ambient Energy 32(2): 95–102.

Arnold, J.N., I. Catton, D.K. Edwards (1976) Experimental investigation of natural convection in inclined rectangular regions of differing aspect ratios. Journal of Heat Transfer 98(1): 67–71.

Bodenshatz, E., W. Pesh, G. Ahlers (2000) Recent developments in Rayleigh-Bénard convection. Annual review of fluid mechanics 32(1): 709–778.

Boussinesq, J. (1903) Théorie Analytique de la Chaleur. Vol. 2, Gauthier-Villars, Paris.

Catton, I. (1978) Natural convection in enclosures. Proceedings of the sixth international heat transfer conference, Vol. 6, pp. 13-31.

Chang, B.H. (2014) Numerical study of flow and heat transfer in differentially heated enclosures. Thermal Science 18(2): 451-463.

Corcione, M. (2003) Effect of thermal boundary conditions at the sidewalls upon natural convection in rectangular enclosures heated from below and cooled from above. International Journal of Thermal Sciences 42(2): 199-208.

Elsherbiny, S.M., G.D. Raithby, K.G.T. Hollands (1982) Heat transfer by natural convection across vertical and inclined air layers. Journal of Heat Transfer 104(1): 96-102.

Elsherbiny, S.M (1996) Free convection in inclined air layers heated from above. International journal of heat and mass transfer 39(18): 3925-3930.

Hamady, F.J., J.R. Lloyd, H.Q. Yang, K.T. Yang (1989) Study of local natural convection heat transfer in an inclined enclosure. International Journal of Heat and Mass Transfer 32(9): 1697-1708.

Hart, E.J. (1971) Stability of the flow in differentially heated inclined box. Journal of Fluid Mechanics 47(3): 547-576.

Hollands, K.G.T., L. Konicek (1973) Experimental study of the stability of differentially heated inclined air layers. International Journal of Heat and Mass Transfer 16(7): 1467-1476.

Huppert, H.E., J.S. Turner (1981) Double-diffusive convection. Journal of Fluid Mechanics 106: 299-329.

Jaluria, Y. (1980) Natural Convection Heat and Mass Transfer, Oxford, Pergamon Press.

Khezzar, L., D. Siginer, I. Vinogradov (2012) Natural convection in inclined two dimensional rectangular cavities. Heat and Mass Transfer 48(2): 227-239.

Labed, A., A. Aliouali, K. Aoues, M. Zellouf (2005) Etude numérique de la convection naturelle thermosolutale bidimensionnelle dans une enceinte fermée, Journées d'Etudes Nationale de La Mécanique, Ouargla.

Labed, A., N. Moummi, A. Benchabane, K. Aoues, A. Moummi (2012) Performance investigation of single-and double-pass solar air heaters through the use of various fin geometries. International Journal of Sustainable Energy 31(6): 423-434.

Labed, A., N. Moummi, K. Aoues, M. Zellouf (2013) Etude expérimentale des performances thermiques et des pertes de charges de différentes configurations de capteurs solaires plans à air, 16ème Edition des Journées Internationales de Thermique, Marrakech.

Labed, A., N. Moummi, M. Zellouf, K. Aoues, A. Rouag (2014) Effect of different parameters on the solar drying of henna; experimental investigation in the region of Biskra (Algeria). 13th Int. conference on clean energy, Istanbul.

Labed, A., A. Rouag, A. Benchabane, N. Moummi, M. Zerouali (2015) Applicability of solar desiccant cooling systems in Algerian Sahara: Experimental investigation of flat plate collectors. Journal of Applied Engineering Science & Technology, 1 (2): 61-69.

Moummi, N., S. Youcef-Ali, A. Moummi, J.Y. Desmons (2004) Energy analysis of a solar air collector with rows of fins. Renewable Energy 29(13) 2053,2064.

Moummi, N., A. Moummi, K. Aoues, C. Mahboub, S. Youcef-Ali (2010) Systematic forecasts of solar collector's performance in various sites of different climates in Algeria. International journal of sustainable energy 29(3): 142–150.

Oberbeck, A. (1879) Über die, Wärmeleitung der Flüssigkeiten bei Berücksichtigung der Strömungen infolge von Temperatur-differenzen. Annalen der Physik 243(6), 271-292.

Ostrach, S. (1972) Natural convection in enclosures. Advances in heat transfer 8, 161-227.

Ozoe, H., H. Sayama, S.W. Churchill (1975) Natural convection in an inclined rectangular channel at various aspect ratios and angles – experimental measurements. International Journal of Heat and Mass Transfer 18(12): 1425-1431.

Patankar, S.V., D.B. Spalding (1972) A calculation procedure for heat, mass and momentum transfer in three-dimensional parabolic flows. International journal of heat and mass transfer 15(10): 1787-1806.

Patankar, S.V. (1980) Numerical heat transfer and fluid flow. McGraw-Hill, New York.

Soong, C.Y., P.Y. Tzeng, D.C. chiang, T.S. Sheu (1996) Numerical study on mode-transition of natural convection in differentially heated inclined enclosures. International Journal of Heat and Mass Transfer 39(14): 2869-2882.

Turner, J.S. (1985) Multicomponent convection. Annual Review of Fluid Mechanics 17(1): 11-44.

Van Doormaal, J.P., G.D. Raithby (1984) Enhancement of the simple method for predicting incompressible fluid flow. Numerical heat transfer 7(2): 147-163.

Wang, H., M.S. Hamed (2006) Flow mode-transition of natural convection in inclined rectangular enclosures subjected to bidirectional temperature gradients. International journal of thermal sciences 45(8): 782-795.

Zellouf, M., N. Moummi, K. Aoues, A. Labed (2014) Numerical study on heat transfer and flow mode-transition of natural convection in inclined cavity. Proceedings of 2nd Int. Conference on Applied Energetic and Pollution, Constantine, Vol. 2, pp. 524-532.

Zeytounian, R.K. (2003) Joseph Boussinesq and his approximation: a contemporary view. Comptes Rendus Mecanique 331(8): 575-586.